Journal of Molecular Structure 1056–1057 (2014) 267–272

Contents lists available at ScienceDirect

Journal of Molecular Structure

journal homepage: www.elsevier.com/locate/molstruc

A vibrational spectroscopic study of the arsenate mineral bayldonite $(Cu,Zn)_3Pb(AsO_3OH)_2(OH)_2$ – A comparison with other basic arsenates

Ray L. Frost [a,*], Andrés López [a], Guilherme de Oliveira Gonçalves [b], Ricardo Scholz [b], Yunfei Xi [a]

[a] School of Chemistry, Physics and Mechanical Engineering, Science and Engineering Faculty, Queensland University of Technology, GPO Box 2434, Brisbane, Queensland 4001, Australia
[b] Geology Department, School of Mines, Federal University of Ouro Preto, Campus Morro do Cruzeiro, Ouro Preto, MG 35400-00, Brazil

HIGHLIGHTS

- We have studied a hydroxy arsenate of copper and lead of formula $Cu_3Pb(AsO_3OH)_2(OH)_2$.
- Raman and infrared bands are attributed to the vibrational modes of $(AsO_4)^{3-}$ and $(HOAsO_3)^{2-}$ units.
- A comparison is made with spectra of the other basic copper arsenate minerals.

GRAPHICAL ABSTRACT

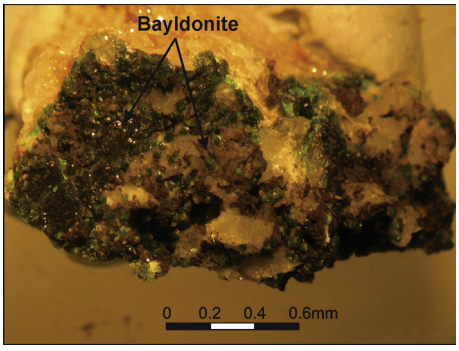

ARTICLE INFO

Article history:
Received 24 July 2013
Received in revised form 9 October 2013
Accepted 10 October 2013
Available online 24 October 2013

Keywords:
Bayldonite
Arsenate
Raman spectroscopy
Hydroxyl
Olivenite

ABSTRACT

We have studied the vibrational spectra of the mineral bayldonite, a hydroxy arsenate of copper and lead of formula $Cu_3Pb(AsO_3OH)_2(OH)_2$ from the type locality, the Penberthy Croft Mine, St Hilary, Mount's Bay District, Cornwall, England and relate the spectra to the mineral structure. Raman bands at 896 and 838 cm^{-1} are assigned to the $(AsO_4)^{3-}$ ν_1 symmetric stretching mode and the second to the $(AsO_4)^{3-}$ ν_3 antisymmetric stretching mode. It is noted that the position of the symmetric stretching mode is at a higher position than the antisymmetric stretching mode. It is proposed that the Raman bands at 889 and 845 cm^{-1} are symmetric and antisymmetric stretching modes of the $(HOAsO_3)^{2-}$ units. Raman bands of bayldonite at 490 and 500 cm^{-1} are assigned to the $(AsO_4)^{3-}$ ν_4 bending modes. Raman bands for bayldonite are noted at 396, 408 and 429 cm^{-1} and are assigned to the $(AsO_4)^{3-}$ ν_2 bending modes. A comparison is made with spectra of the other basic copper arsenate minerals, namely cornubite, olivenite, cornwallite.

1. Introduction

The mineral bayldonite is a hydroxy arsenate of copper and lead of formula $Cu_3Pb(AsO_3OH)_2(OH)_2$ [1,2]. Some substitution of Cu by Pb and/or Ni may be found [3–5]. Bayldonite occurrence is related to oxidation zone in Cu–Pb–Zn deposits [6], associated with secondary phosphates and arsenates, like in the Black Pine mine (Philipsburg, Montana, USA) [7], Tsumeb (SW Africa), France (Verriere, Ardillats, Róhe, Rebasse, Ceilhes, Herault), in an uranium mine in England (Grampound Road, Cornwall) [8]. Bayldonite also occurs associated in barite lenses embedded in sandstones in metassomatic Pb–Zn deposits in Kayrakty, in central Kazakhztan [9] and in conglomerates related to quartz-barite veins of the Capitana mine, Chile [10]. In Australia, it was found in the Anticline prospect, 11 km west-southwest of Ashburton Downs homestead, Capricorn Range, Western Australia and at the Mt. Malvern mine, near Clarendon, South Australia. The mineral is found in many parts of the world [3,11–17] and is also supposedly formed by alteration of enargite (Lattanzi et al., and references therein [18]).

* Corresponding author. Tel.: +61 7 3138 2407; fax: +61 7 3138 1804.
E-mail address: r.frost@qut.edu.au (R.L. Frost).

0022-2860/$ - see front matter © 2013 Elsevier B.V. All rights reserved.
http://dx.doi.org/10.1016/j.molstruc.2013.10.030

In recent studies, $Ba[Co_3(VO_4)_2(OH)_2]$ with a regular Kagomé lattice was synthesised under low-temperature hydrothermal conditions and have a structure that is topologically related to bayldonite [19].

Arsenate minerals, such as bayldonite, are a major concern when related to environmental problems especially when it comes to mining and metallurgical wastes. In order to understand the solubility conditions, Magalhães and Silva (and references therein [5]) calculated the *Gibbs* energy of formation of bayldonite, at 298 K, as 1810.6 kJ mol^{-1} and Vaca-Escobar et al. (and references therein [20]), proved that the formation of a highly-insoluble heavy metal arsenates (such as bayldonite) is the predominant immobilization mechanism, over adsorption processes.

The crystal structure of bayldonite was determined by different authors [8,9,21]. The mineral is monoclinic with point group 2/*m*. The cell data is *Space Group: C*2/*c*, $a = 10.147(2)$ Å, $b = 5.892(1)$ Å, $c = 14.081(2)$ Å and $z = 4$. Bayldonite structure contains adjacent sheets of Cu^{2+} (Φ_6) octahedral and AsO_4 tetrahedra connected through irregular Pb^{2+} (Φ_8) polyhedra and hydrogen bonding, with (2 + 2 + 2)-distorted Cu^{2+} (Φ_6) octahedra, as a result of a dynamic Jahn-Teller effect [9,22]. Burns and Hawthorne and Sumín de Portilla et al. showed that the empirical formula proposed by Guillemin [8] $PbCu_3(AsO_4)_2(OH)_2$, was incorrect and they proposed the formula $Cu_3PbO(HOAsO_3)_2{\cdot}(OH)_{2-}$ [9,22]. Magalhães and Silva (and references therein [5]) refer to bayldonite crystallographic system as triclinic. According to Ghose and Wan [4], the structure of bayldonite consists of interconnected Cu octahedral layers and Pb arsenate polyhedral–tetrahedral layers which alternate along the *c* axis, giving rise to complex pseudo-hexagonal layers parallel to (0 0 1).

Bayldonite is one of many basic copper minerals containing arsenate anion [6]. There exists a number of dark emerald green copper arsenate minerals, including olivenite $[Cu_2(AsO_4)_2(OH)]$, cornwallite $[Cu_5(AsO_4)_2(OH)_4]$ and clinoclase $[Cu_3(AsO_4)(OH)]$ [23]. Each of these minerals occurs in the oxidized zones of copper deposits [6] and olivenite is by far the commonest [23]. The stability of the basic copper arsenate minerals is related to their redox potential and phase fields exist for the related minerals olivenite, cornubite, clinoclase and cornwallite. The mineral structure of olivenite is monoclinic, pseudo-orthorhombic with point group *2*/*m* [24,25]. The mineral has a space group of $P2_1/n$. Cornwallite is monoclinic with point group: *2*/*m* and space group $P2_1/a$ [24,26]. Clinoclase is also monoclinic with point group *2*/*m* and space group $P2_1/a$ [26,27]. Thus the structure of these three phase related minerals are related and should provide related spectra, which should only differ in terms of the intensity of the bands according to the relative mole ratios of Cu/As/OH.

The objective of this research is to report the Raman and infrared spectra of bayldonite and to relate the vibrational spectra to the mineral structure.

2. Experimental

2.1. Samples description and preparation

The bayldonite sample studied in this work forms part of the collection of the Geology Department of the Federal University of Ouro Preto, Minas Gerais, Brazil, with sample code SAC-089. The studied sample is from the type locality, the Penberthy Croft Mine, St Hilary, Mount's Bay District, Cornwall, England.

The sample was gently crushed and the associated minerals were removed under a stereomicroscope Leica MZ4. The bayldonite studied in this work occurs in association with siderite. Scanning electron microscopy (SEM) in the EDS mode was applied to support the mineral characterization.

Cornwallite and olivenite from the Penberthy Croft Mine, St Hilary, Cornwall, UK, were supplied by Mr. John Betterton. Samples of olivenite and clinoclase from the Tin Stope, Majuba Hill mine, Utah, USA, were purchased from the Mineralogical Research Company. All were checked for purity by powder X-ray diffraction and by SEM and microprobe methods. Negligible amounts of phosphorus or transition metals other than copper were found in the samples used for this spectroscopic study.

2.2. Scanning electron microscopy (SEM)

Experiments and analyses involving electron microscopy were performed in the Center of Microscopy of the Universidade Federal de Minas Gerais, Belo Horizonte, Minas Gerais, Brazil (http://www.microscopia.ufmg.br).

Bayldonite crystals were coated with a 5 nm layer of evaporated carbon. Secondary Electron and Backscattering Electron images were obtained using a JEOL JSM-6360LV equipment. Qualitative and semi-quantitative chemical analyses in the EDS mode were performed with a ThermoNORAN spectrometer model Quest and were applied to support the mineral characterization.

2.2.1. Raman spectroscopy

The crystals of bayldonite and other basic copper arsenates were placed and oriented on the stage of an Olympus BHSM microscope, equipped with 10× and 50× objectives and part of a Renishaw 1000 Raman microscope system, which also includes a monochromator, a filter system and a Charge Coupled Device (CCD). Raman spectra were excited by a HeNe laser (633 nm) at a nominal resolution of 2 cm^{-1} in the range between 100 and 4000 cm^{-1}. Details of the experimental procedure have been published [28–30]. The spatial resolution of the instrument is 1 μm. Thus, if crystals are less than this value, a mixture of crystals will be measured. However, the crystals of bayldonite used in this experiment were >1.1 μm.

Spectral manipulation such as baseline adjustment, smoothing and normalisation were performed using the Spectracalc software package GRAMS (Galactic Industries Corporation, NH, USA). Band component analysis was undertaken using the Jandel 'Peakfit' software package which enabled the type of fitting function to be selected and allows specific parameters to be fixed or varied accordingly. Band fitting was done using a Lorentz–Gauss cross-product function with the minimum number of component bands used for the fitting process. The Gauss–Lorentz ratio was maintained at values greater than 0.7 and fitting was undertaken until reproducible results were obtained with squared correlations of r^2 greater than 0.995.

3. Results and discussion

3.1. Chemical characterization

The SEM image of balydonite sample studied in this work is shown in Fig. 1. Balydonite crystals show a tetragonal form and the crystal aggregate forms a rosette habitus. Qualitative chemical composition shows a homogeneous phase, composed by Cu, Pb, C and As, with minor amounts of Al (Fig. 2). (The carbon is from the carbon coating).

3.1.1. Spectroscopy of the arsenate anion

The arsenate ion, $(AsO_4)^{3-}$, is a tetrahedral unit with T_d symmetry and exhibits four fundamental vibrations: (i) the symmetric stretching vibration ν_1 (A_1) (818 cm^{-1}), (ii) the doubly degenerate bending vibration ν_2 (E) (350 cm^{-1}), (iii) the triply degenerate antisymmetric stretching vibration ν_3 (F_2) (786 cm^{-1}), and (iv)

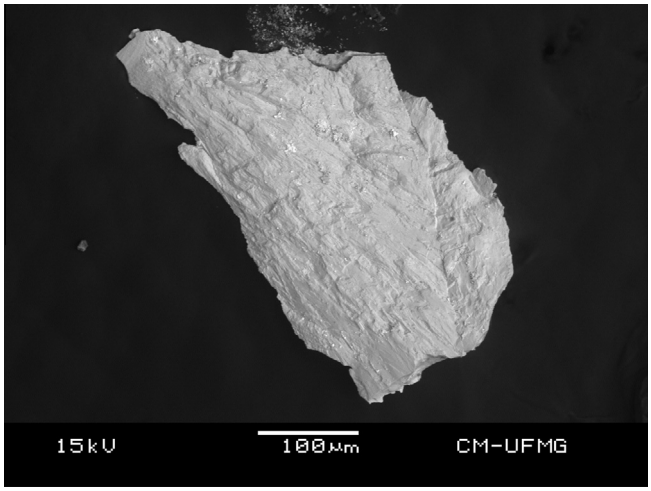

Fig. 1. Backscattered electron image (BSI) of a bayldonite fragment up to 0.5 mm in length.

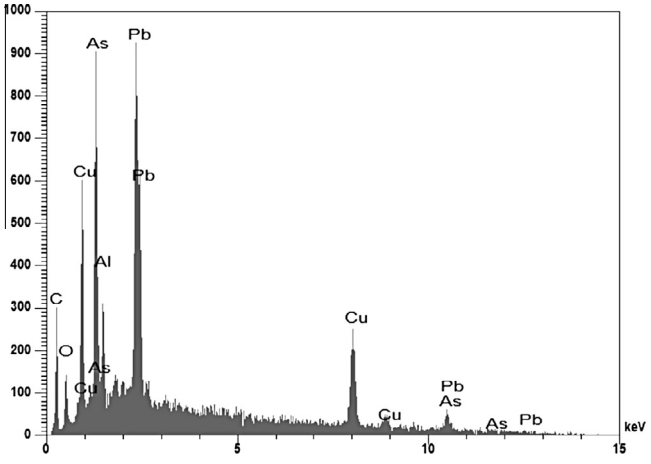

Fig. 2. EDS analysis of bayldonite.

the triply degenerate bending vibration ν_4 (F_2) (398 cm^{-1}). The F_2 modes are Raman and infrared active, whereas A_1 and E modes are Raman active only. According to Frost et al., [28–30], the ν_1 $(AsO_4)^{3-}$ vibration may coincide with the ν_3 $(AsO_4)^{3-}$ vibration. It should be noted that the wavenumber of the ν_1 $(AsO_4)^{3-}$ may be greater than that of the ν_3 $(AsO_4)^{3-}$, which is an inversion of the normal behavior shown by most tetrahedral ions, although such an inversion is not unique [31,32]. According to Myneni et al. [33], the T_d symmetry of $(AsO_4)^{3-}$ unit is rarely preserved in minerals and synthetic compounds, because of its strong affinity to protonate, hydrate, and complex with metal ions. Such chemical interactions reduce $(AsO_4)^{3-}$ tetrahedral symmetry to either C_{3v}/C_3 (corner sharing), C_{2v}/C_2 (edge-sharing, bidentate binuclear), or C_1/C_s (corner sharing, edge-sharing, bidentate binuclear, multidentate]. This symmetry lowering is connected with activation of all vibrations in infrared and Raman spectra and splitting of doubly and triply degenerate vibrations. Nine normal modes may be Raman and infrared active in the case of the lowest C_s symmetry [34].

3.1.2. Vibrational spectroscopy of bayldonite

The Raman spectrum over the 100–4000 cm^{-1} spectral range is shown in Fig. 3a. This figure demonstrates the position and relative intensity of the Raman bands. It is noted that there are large parts of the spectrum where little or no intensity is observed. Therefore,

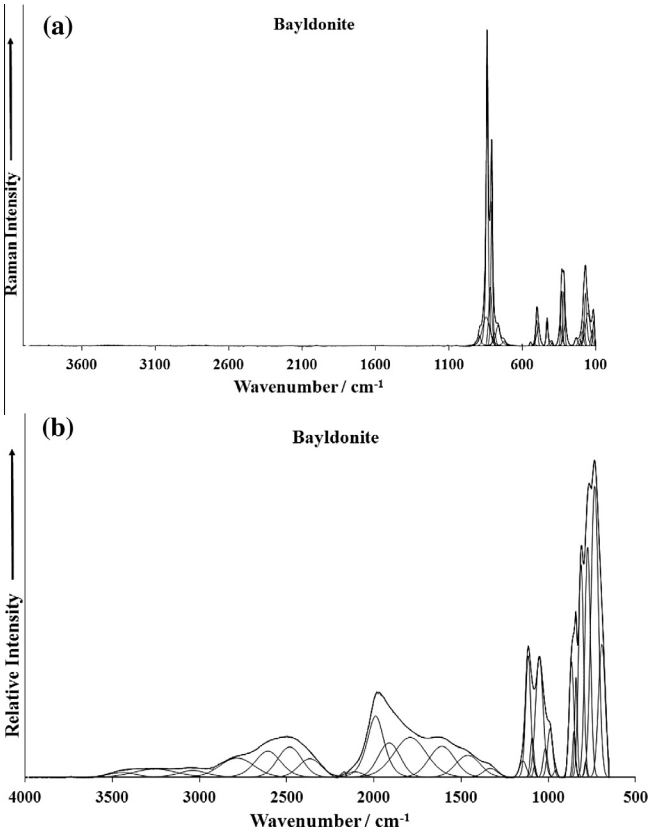

Fig. 3. (a) Raman spectrum of bayldonite (upper spectrum) and (b) infrared spectrum of bayldonite (lower spectrum).

the spectrum is subdivided into sections based upon the type of vibration being studied. The infrared spectrum of bayldonite over the 500–4000 cm^{-1} spectral range is given in Fig. 3b. This spectrum may also be subdivided into sections based upon the type of vibration being studied.

The Raman spectrum of bayldonite in the 650–950 cm^{-1} spectral range is reported in Fig. 4a. The spectrum is characterised by two intense Raman bands at 896 and 838 cm^{-1}. The first band is assigned to the $(AsO_4)^{3-}$ ν_1 symmetric stretching mode and the second to the $(AsO_4)^{3-}$ ν_3 antisymmetric stretching mode. Two broadish bands at 889 and 845 cm^{-1} are observed. The possible assignment of these bands is to the AsO symmetric and antisymmetric stretching modes of the $(HOAsO_3)^{2-}$ units. In the spectra reported here, the B_g modes occur at lower wavenumbers than the A_g modes. Normally the antisymmetric stretching modes occur at higher wavenumbers than the symmetric stretching modes, however sometimes when atoms of large atomic mass are involved; the position of the bands can be the other way around. In the Raman spectrum of bayldonite given in the RRUFF data base, two Raman bands are observed at 803 and 836 cm^{-1} (please see the figure given in the Supplementary information). A comparison of the results of the Raman spectrum of balydonite with that of olivenite, cornwallite and clinoclase is given in Table 1.

For each basic copper arsenate mineral, two bands are observed in the 298 K spectra. Olivenite shows two bands at 853 and 820 cm^{-1}, Cornwallite at 859 and 806 cm^{-1}, cornubite at 815 and 780 cm^{-1} and clinoclase at 823 and 771 cm^{-1}. By scale expansion of the *Y*-axis for olivenite, additional very weak bands are observed at 880 and 790 cm^{-1}. The most intense band is assigned to the $\nu_1(A_1)$ symmetric stretching vibration. This assignment differs from that described by Sumin de Portilla [35]. In this work, the $\nu_3(F_2)$ mode was described as splitting into four components at

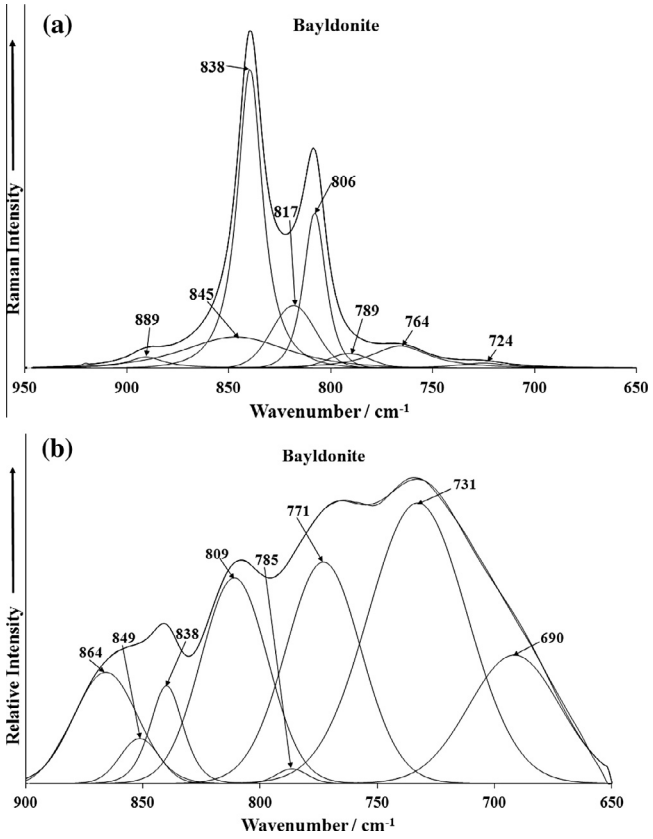

Fig. 4. (a) Raman spectrum of bayldonite (upper spectrum) in the 800–1400 cm^{-1} spectral range and (b) infrared spectrum of bayldonite (lower spectrum) in the 500–1300 cm^{-1} spectral range.

870, 830, 800 and 750 cm^{-1}. Farmer suggested that the ν_1 and ν_3 modes overlapped and were to be found at the same frequency [36]. Whilst this is highly unusual, we suggest that the two vibrations at 853 and 820 cm^{-1} are the AsO symmetric and antisymmetric stretching vibrations respectively. Griffith reported the Raman spectrum of olivenite [37]. Raman bands were found at 880 ($A^{|}$), 856 (B_{2u}), 810 ($A^{|}$) and 790 (B_{2u}) cm^{-1}. The observation of the bands 853 and 820 cm^{-1} is in good agreement with the data published by Griffith [37]. Bands at 880 and 790 cm^{-1} are in excellent agreement with the data of Griffith [37]. The most intense bands in the Raman spectra are the bands at 853 and 810 cm^{-1}.

The infrared spectrum of bayldonite in the 650–900 cm^{-1} spectral range is shown in Fig. 4b. The spectrum is very broad and a series of infrared bands may be resolved at 690, 731, 771, 809, 838, 849 and 864 cm^{-1}. The two infrared bands at 838 and 809 cm^{-1} may be assigned to the $(AsO_4)^{3-}$ ν_1 symmetric stretching mode and the second to the $(AsO_4)^{3-}$ ν_3 antisymmetric stretching mode. It is noted that the intensity of these two infrared bands is the inverse of the intensity of the two Raman bands at the equivalent peak positions. The two infrared bands at 864 and 849 cm^{-1} may be attributed to the As–O symmetric and antisymmetric stretching modes of the $(HOAsO_3)^{2-}$ units. The other infrared bands at 731 and 771 cm^{-1} are attributed to the deformation modes of the hydroxyl units.

The Raman spectrum of bayldonite in the 250–550 cm^{-1} spectral range is displayed in Fig. 5a. The spectrum of this spectral region of bayldonite may be divided into three separate regions: (a) 450-650 cm^{-1} (b) 400–450 cm^{-1} and (c) 400–250 cm^{-1}. It is proposed that these three regions define the (a) ν_4 modes (b) ν_2 modes and (c) AsO bending and lattice modes. The ν_2 bending vibration should be common to the spectra of all the basic copper arsenates and should be intense. Raman bands of bayldonite are observed at 490 and 500 cm^{-1} with a low intensity shoulder at 514 cm^{-1} and are assigned to the $(AsO_4)^{3-}$ ν_4 bending modes. Raman bands for bayldonite are noted at 396, 408 and 429 cm^{-1} and are assigned to the $(AsO_4)^{3-}$ ν_2 bending modes. The series of bands at 316 and 330 cm^{-1} with both higher and lower wavenumber shoulders are assigned to metal oxygen stretching vibrations (CuO and PbO).

A comparison may be made with the other basic copper arsenate minerals. In the Raman spectrum of olivenite, a series of bands are observed at 632, 590, 554 and 513 cm^{-1}. These bands are attributed to the ν_4 mode of arsenate. Infrared bands were observed by Sumin de Portilla [35] at 492, 452 and 400 cm^{-1} with a fourth component predicted to be below 400 cm^{-1}. No comparison can be made between the infrared data and these Raman results although a closer comparison with the Raman results for this spectral region of cornwallite exists. The Raman spectrum of cornwallite displays bands at 603, 536, 509, 446 and 416 cm^{-1}. For clinoclase Raman bands are observed at 607, 539, 508, 482 and 460 cm^{-1}, which are more in harmony with the Raman data for olivenite. Reduction in site symmetry would be the cause of additional bands in this region. A band at 545 cm^{-1} was observed in the infrared spectrum of olivenite and it was suggested that this was a CuO stretching vibration [35]. However a band in this position seems too high for this type of vibration. We propose that the bands in these positions are attributable to the ν_4 vibrational modes and the number of bands is due to the loss of degeneracy.

Table 1
Results of the Raman spectroscopic analysis of balydonite, olivenite, cornwallite and clinoclase.

Olivenite			Cornwallite	Clinoclase	Balydonite	
Raman/cm^{-1}	Published data [14,17]/cm^{-1} Infrared	Published data [14,17]/cm^{-1} Raman	Raman/cm^{-1}	Raman /cm^{-1}	Raman /cm^{-1}	Suggested assignments
3464	3580 [14]		3411	3559	Not observed	OH stretches
3437	3440		3350	3339		
957	950 [14]		962	983	962	OH deforms
853	860	880 [17]	877			
	828	856	859	850	896	ν_1 & ν_3
819	790	790	806	832	838	
			763	783		
360			363	348	500	ν_2 & ν_4
346			347	318	490	
335		324	330	308	429	
		310			408	
					396	
	1082		1087		Not observed	Overtones or impurity
	1037					
	938					

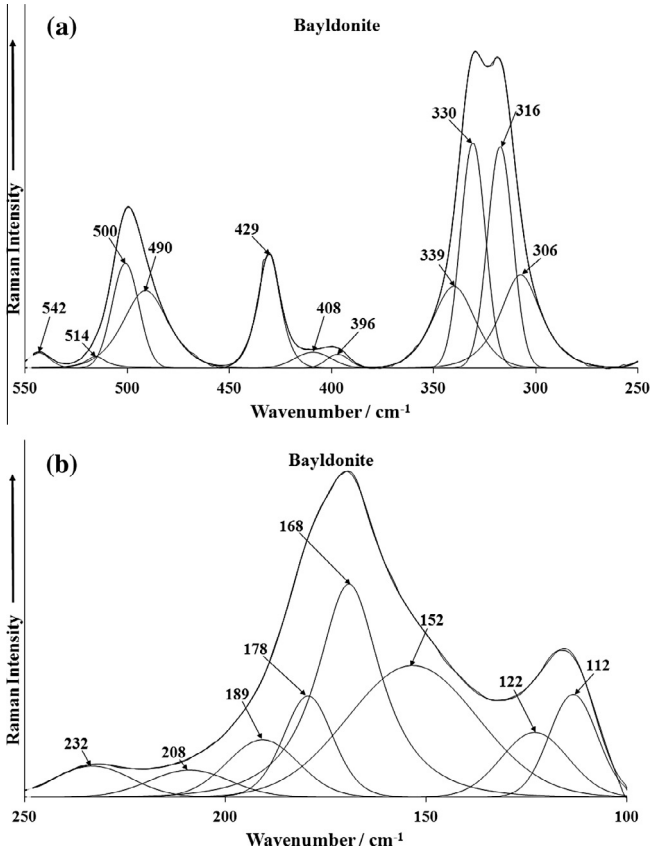

Fig. 5. (a) Raman spectrum of bayldonite (upper spectrum) in the 250–550 cm^{-1} spectral range and (b) Raman spectrum of bayldonite (lower spectrum) in the 100–250 cm^{-1} spectral range.

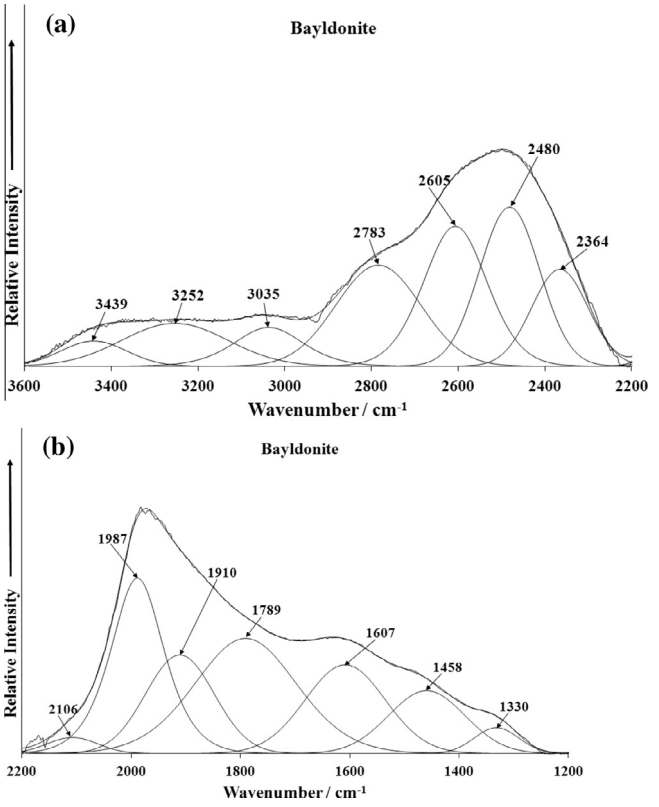

Fig. 6. (a) Infrared spectrum of bayldonite (upper spectrum) in the 2200–3600 cm^{-1} spectral range and (b) Infrared spectrum of bayldonite (lower spectrum) in the 1200–2200 cm^{-1} spectral range.

With vibrational spectroscopic studies of these minerals, two questions arise (a) the position of the hydroxyl deformation vibration and (b) the position of the ν_2 band. Because of the atomic mass of As, it is predicted that the bending modes will be below 400 cm^{-1}. Thus, the region from around to 270 to around 360 cm^{-1} is the region where this vibration is to be observed. In the Raman spectrum of olivenite three bands at 350, 346 and 335 cm^{-1} are observed and we assign these bands to the ν_2 bending modes. For cornwallite, three bands are observed at 363, 347 and 330 cm^{-1} in the 298 K spectrum. These results are consistent with those of olivenite. For clinoclase, Raman bands are observed at 348, 318 and 308 cm^{-1}.

The Raman spectrum of bayldonite in the 100–250 cm^{-1} spectral region is shown in Fig. 5b. The spectrum is quite broad and various component bands may be resolved.

The Raman spectrum of bayldonite in the OH stretching region was not able to be collected. The infrared spectrum of bayldonite in the 2200–3600 cm^{-1} spectral range is displayed in Fig. 6a. The spectrum is quite broad and shows complexity. It is proposed that these bands are due to the stretching vibration of the OH units. The infrared spectrum of bayldonite in the 1200–2200 cm^{-1} spectral range is displayed in Fig. 6b. Again, the spectrum shows complexity with multiple overlapping bands. Diffuse reflectance spectroscopy (DRIFT) spectroscopy indicates no band around 1620 cm^{-1}. Thus, no water is present in this mineral.

The Raman spectra of the hydroxyl-stretching region of olivenite, cornwallite, cornubite and clinoclase were obtained. For olivenite the Raman spectrum may be resolved into two overlapping bands centred upon 3464 and 3437 cm^{-1}. In the spectrum of the hydroxyl-stretching region of cornwallite two partially band-separated peaks are observed at 3411 and 3350 cm^{-1}. For cornubite, two bands are observed at 3324 and 3042 cm^{-1}. For clinoclase two well separated bands separated peaks are observed at 3559 and 3339 cm^{-1}. The observation of two hydroxyl-stretching vibrations means that there are two distinct and different hydroxyl units in the basic copper arsenate minerals. The difference between the peak positions of olivenite and cornwallite is related to the strength of the hydrogen bond formed between the hydroxyl unit and an adjacent arsenate unit. This bonding is much stronger in cornwallite as indicated by the lower wavenumber position of the hydroxyl-stretching vibrations. One interpretation is that the higher wavenumber vibration is ascribed to the As–OH vibration and the lower wavenumber hydroxyl stretching frequency to the As–OH···O vibration.

4. Conclusions

We have studied the vibrational spectra of the mineral bayldonite, a hydroxy arsenate of copper and lead of formula $Cu_3Pb(AsO_3OH)_2(OH)_2$ from the Rapid Creek sedimentary phosphatic iron formation, northern Yukon. Raman bands at 896 and 838 cm^{-1} are assigned to the $(AsO_4)^{3-}$ ν_1 symmetric stretching mode and the second to the $(AsO_4)^{3-}$ ν_3 antisymmetric stretching mode. Raman bands at 889 and 845 cm^{-1} are symmetric and antisymmetric stretching modes of the $(HOAsO_3)^{2-}$ units. Raman bands of bayldonite at 490 and 500 cm^{-1} are assigned to the $(AsO_4)^{3-}$ ν_4 bending modes. Raman bands for bayldonite are noted at 396, 408 and 429 cm^{-1} and are assigned to the $(AsO_4)^{3-}$ ν_2 bending modes. A comparison is made with spectra of the other basic copper arsenate minerals, namely cornubite, olivenite, cornwallite.

The application of Raman microscopy to the study of closely related mineral phases has enabled their molecular characterisation

using their Raman spectra, thus enabling the rapid identification of phases in complex mixtures of secondary copper arsenates from the oxidized zones of base metal ore bodies.

Acknowledgements

The financial and infra-structure support of the Discipline of Nanotechnology and Molecular Science, Science and Engineering Faculty of the Queensland University of Technology, is gratefully acknowledged. The Australian Research Council (ARC) is thanked for funding the instrumentation. The authors would like to acknowledge the Center of Microscopy at the Universidade Federal de Minas Gerais (http://www.microscopia.ufmg.br) for providing the equipment and technical support for experiments involving electron microscopy. R. Scholz thanks to CNPq – Conselho Nacional de Desenvolvimento Científico e Tecnológico (Grant No. 306287/2012-9).

Appendix A. Supplementary material

Supplementary data associated with this article can be found, in the online version, at http://dx.doi.org/10.1016/j.molstruc.2013.10.030.

References

[1] F. Cesbron, H. Vachey, Min. Mag. 39 (1974) 716–718.
[2] M.C.F. Magalhaes, J.D. Pedrosa de Jesus, P.A. Williams, Min. Mag. 52 (1988) 679–690.
[3] M.A.M. Fettel, Sonderband 27 (1975) 249–254.
[4] S. Ghose, C. Wan, Acta Cryst. B35 (1979) 819–823.
[5] M.C.F. Magalhaes, M.C.M. Silva, Monat. Chem. 134 (2003) 735–743.
[6] P.A. Williams, Oxide Zone Geochemistry, Ellis Horwood Ltd., Chichester, West Sussex, England, 1990.
[7] D.R. Peacor, P.J. Dunn, R.A. Ramik, B.D. Sturman, L.G. Zeihen, Can. Min. 23 (1985) 255–258.
[8] C. Guillemin, Bull. Soc. France 79 (1956) 7–95.
[9] V. Sumin de Portilla, M. Portilla Quevedo, V.I. Stepanov, Amer. Min. 66 (1981) 148–153.
[10] A.R. Kampf, I.M. Steele, R.A. Jenkins, Amer. Min. 91 (2006) 1909–1917.
[11] T. Adachi, T. Minakawa, Chigaku Kenkyu 43 (1994) 165–168.
[12] J. Behier, L.A. Villeneuve, Bull. Soc. France 66 (1943) 25–48.
[13] W.D. Birch, A. Van der Heyden, Min. Rec. 19 (1988) 425–436.
[14] G. Brizzi, F. Olmi, C. Sabelli, Riv. Min. It. (1994) 193–206.
[15] G.E. Dunning, J.F. Cooper Jr., Min. Rec. 18 (1987) 413–420.
[16] M. Fengl, J. Jansa, F. Novak, F. Reichmann, Sbornik Geol. Ved. 17 (1981) 107–125.
[17] Y. Li, L. Lai, Dizhi Xuebao 64 (1990) 337–343.
[18] P. Lattanzi, S.D. Pelo, E. Musu, D. Atzei, B. Elsener, M. Fantauzzi, A. Rossi, Earth-Sc. Rev. 66 (2007) 62–88.
[19] T. Dordevic, L. Karanovic, Acta Cryst. C69 (2013) 114–118.
[20] K. Vaca-Escobar, M. Villalobos, A.E. Ceniceros-Gómez, Appl. Geochem. 27 (2013) 2251–2259.
[21] E.S. Larsen, First edition, USGS Bulletin 679 (1921) 45.
[22] P.C. Burns, F.C. Hawthorne, Can. Min. 34 (1996) 1089–1105.
[23] J.W. Anthony, R.A. bideaux, K.W. Bladh, M.C. Nichols, Handbook of Mineralogy Volume IV arsenates, phosphates and vanadates, Mineral Data Publishing, Tuscon, Arizona, USA, 2000.
[24] L.G. Berry, Amer. Min. 36 (1951) 484.
[25] P.C. Burns, F.C. Hawthorne, Can. Min. 33 (1995) 885.
[26] G.F. Claringbull, M.H. Hey, R.J. Davis, Min. Mag. 32 (1959) 1.
[27] S. Ghose, M. Fehlmann, M. Sundaralingam, Acta Cryst. 18 (1965) 777.
[28] R.L. Frost, J.T. Kloprogge, W.N. Martens, J. Raman Spectrosc. 35 (2004) 28–35.
[29] R.L. Frost, W. Martens, P.A. Williams, J.T. Kloprogge, J. Raman Spectrosc. 34 (2003) 751–759.
[30] W.N. Martens, R.L. Frost, J.T. Kloprogge, P.A. Williams, Amer. Min. 88 (2003) 501–508.
[31] F.K. Vansant, B.J.V.d. Veken, H.O. Desseyn, J. Mol. Struct. 15 (1973) 425–437.
[32] R.H. Busey, O.L. Keller, J. Chem. Phys. 41 (1964) 215–225.
[33] S.C.B. Myneni, S.J. Traina, G.A. Waychunas, T.J. Logan, Geochim. Cosmochim. Acta 62 (1998) 3285–3300.
[34] S.D. Ross, Phosphates and other oxy-anions of group V, in: V.C. Farmer (Ed.), The Infared Spectra of Minerals, Mineralogical Society, London, 1974.
[35] V.I.S.D. Portilla, Can. Min. 12 (1974) 262.
[36] V.C. Farmer, The Infrared Spectra of Minerals, Mineralogical Society London, 1974.
[37] W.P. Griffith, J. Chem. Soc. (1970) 286–291.